



**Repositorio Institucional de la Universidad Autónoma de Madrid**

<https://repositorio.uam.es>

Esta es la **versión de autor** del artículo publicado en:  
This is an **author produced version** of a paper published in:

Chemical Engineering Journal 231 (2013): 172-181

**DOI:** <https://doi.org/10.1016/j.cej.2013.07.005>

**Copyright:** © 2013 Elsevier B.V. All rights reserved

El acceso a la versión del editor puede requerir la suscripción del recurso

Access to the published version may require subscription

# DEVELOPMENT OF POROSITY UPON PHYSICAL ACTIVATION OF GRAPE SEEDS CHAR BY GAS PHASE OXYGEN CHEMISORPTION-DESORPTION CYCLES

*Diana Jimenez-Cordero, Francisco Heras\*, Noelia Alonso-Morales, Miguel A. Gilarranz, Juan J. Rodriguez*

S.D. Ingeniería Química. Universidad Autónoma de Madrid.  
Ctra. Colmenar Viejo, km 15. 28049 Madrid (Spain)

## Abstract

Activation of grape seeds char upon cyclic oxygen chemisorption-desorption permits a controlled development of porosity versus burn-off using air as a cheap activation agent. In this work the influence of chemisorption and desorption temperature and the number of cycles is investigated. A fast increase of BET surface area ( $S_{\text{BET}}$ ) is obtained in the two first cycles; that increase becomes then lower although the  $S_{\text{BET}}$  continues increasing upon the successive cycles. Regarding the Dubinin-Astakhov surface area ( $S_{\text{DA}}$ ) a slow increase was observed from cycle to cycle. The activation process led to the development of both micro and mesoporosity. Under the optimum conditions for surface area development, i.e. an oxidation temperature of 275°C and desorption temperatures between 850 and 950°C, values of 1129-1256 and 1339-1219 m<sup>2</sup>/g were obtained for  $S_{\text{BET}}$  and  $S_{\text{DA}}$ , respectively. Porosity was found to increase mainly during the desorption stage, although chemisorption also led to some surface area development. SEM characterization showed that the activated carbon maintained the granular morphology of the seeds even after 10 cycles showing the egg-shell structure of the precursor with longer and deeper cracks at the outer surface. The activated carbons showed a good mechanical strength during attrition tests.

**Keywords:** Biomass; Activated carbon; Physical activation; Cyclic activation;

## 1 Introduction

The use of agricultural by-products or wastes as precursors for the preparation of activated carbon can reduce substantially the production cost providing a route for

\* Corresponding author Tel.: +34 914978051; fax: +34 914972981.

E-mail address: fran.heras@uam.es

valorization [1]. There are a variety of seed-containing fruits that have been considered for the preparation of activated carbons. However, little attention has been paid so far to grape seeds, even though they represent up to 15% of the solid wastes from the wine industry [2, 3].

In physical activation the most commonly used activating agents are CO<sub>2</sub> and steam. Although air (oxygen) is by far the least expensive option, it is barely used because of its high reactivity that makes difficult an effective control of the activation process. Thus, activation with air most commonly takes place under diffusion control leading to particle burn-off with a poor development of surface area. Cyclic activation by oxygen chemisorption-desorption has been proposed as an interesting solution for a controlled activation that allows tailoring the activated carbons through targeted porosity development [4,5]. Cyclic oxygen chemisorption-desorption consists of a chemisorption step at low temperature followed by desorption in an inert atmosphere at high temperature. The sequence is repeated until a convenient development of porosity is achieved. This method, so far scarcely studied in the literature, can provide an efficient way to create whole porosity from a precursor and to controllably modify the porous structure of a carbonaceous material while maintaining the physical integrity of the particle so that granular activated carbon can be obtained.

This method is a feasible alternative to the traditional one-step or two-stage process for the production of activated carbon. Knowledge of the effects of different operating variables during carbonization and the activation process is important for controlling the porosity and the physical integrity of the final product [1].

The objective of this work is to study the influence of the chemisorption and desorption temperature and the number of activation cycles in the development of porosity during the activation of grape seeds char by cyclic oxygen chemisorption-desorption, using air as oxygen source. In a former work the pyrolysis conditions were optimized in order to obtain a starting char maintaining the granular morphology of the grape seed and develop an incipient microporosity that can favor further activation [6]. The aim is to learn on the compromise between burn-off, porosity and particle integrity so that the resulting material can be used as a granular adsorbent, being the activation by chemisorption-desorption cycles characterized by low burn-off values.

## 2. Material and Methods

The raw material used in this study were seeds collected from grapes of the red variety “Tinta de Toro” harvested for red wine manufacture in Toro (Zamora, Spain). The seeds were washed, dried and then extracted with hexane to remove essential oil before pyrolysis [6]. The oil content of grape seeds depends on the grape variety, though usually ranges between 10 and 16% weight on a dry basis [2]. In our work it amounted 9%. The char used as starting material was obtained by flash pyrolysis of the extracted seeds at 800°C, according to the results of a previous work [6]. The char yield was 34% of the extracted seeds weight on a dry basis. The elemental composition of char was 85.6, 1.0, 1.7 and 0.04% of C, H, N and S, respectively, and the ash content was 8% [6].

### 2.1 *Samples characterization*

Prior to the study of activation cycles, isothermal and non isothermal thermogravimetric analyses (TGA) of the char were carried out with a Mettler SDTA851<sup>e</sup> apparatus in order to establish the temperature ranges for the chemisorption and desorption steps of the activation cycle. The gas flow (N<sub>2</sub>) was 100NmL/min, whereas the heating rate was 10°C/min. In the isothermal chemisorption the nitrogen flow was maintained during heating until the working temperature was achieved. The effect of chemisorption and desorption temperature in the distribution of surface functional groups was studied by temperature programmed desorption (TPD). The samples (100mg) were heated from 100 to 900°C at a rate of 10°C/min under a nitrogen flow of 100NmL/min and the CO and CO<sub>2</sub> evolved were monitored using a Siemens Ultramat 22 detector.

The elemental composition of char (C, N, H and S) was analyzed by a LECO CHNS-932 apparatus. The ash mass fraction of the char was determined by calcinations at 800 °C in a crucible for 2 h. Surface area and total pore volume of the samples were measured in an automated volumetric gas adsorption Micromeritics apparatus (Tristar 3020) by adsorption of N<sub>2</sub> at 77K, and CO<sub>2</sub> at 273K. Approximately 0.15 g of sample

was used in each test. Samples were placed in a glass container and degassed at 150°C during 7h prior to the adsorption measurements using a Micromeritics sample degas system (VacPrep 061). The N<sub>2</sub> adsorption-desorption isotherms were obtained in the 10<sup>-5</sup> – 1.0 P/P<sub>0</sub> range, although the P/P<sub>0</sub> range used to calculate the BET surface area (S<sub>BET</sub>) was 0.05 – 0.3 [7]. The t-method was used for the micropore volume and BJH was used to obtain the mean mesopore size, whereas Dubinin-Astakhov (DA) model was applied to the CO<sub>2</sub> isotherms to determine the DA surface area (S<sub>DA</sub>), micropore volume and mean micropore size [8]. The Non-Local Density Functional Theory (NLDFT) with pore geometry slit was used to calculate the pore size distribution from both the CO<sub>2</sub> and N<sub>2</sub> isotherms [9].

The morphology of grape seeds char and activated carbons was analyzed by Scanning Electron Microscopy (SEM). The SEM analysis was performed using a Hitachi S-3000N apparatus. The specimens for SEM observation were metalized with gold to prevent electrical charging during examination using a Sputter Coater SC502. Imaging was done in the high vacuum mode under an accelerating voltage of 20kV, using secondary electrons. To obtain samples of the outer layer of activated carbons, the carbons were subjected to attrition on a sieve (1mm opening) in a Orto Alresa sifter at a stirring velocity of 2500rpm.

## 2.2 Cyclic activation

The activation of all the samples was carried out in a vertical quartz tube (70 cm length and 3.5 cm width) placed in a sandwich-type electrical furnace under controlled heating rate, temperature and gas flow using PID controllers and mass flow meters. After each activation cycle the reactor was cooled under nitrogen flow and the activated carbon was collected to estimate the burn-off and perform the textural characterization. Burn-off values were referred to the initial char weight and describe the accumulated loss of weight for the number of cycles considered. The chemisorption step of each cycle was tested at three different temperatures (200, 250 and 275°C) for 2h under a 100NmL/min air flow. The desorption step was carried out at four different temperatures (500, 675, 850 and 950°C) using a flow rate of 100NmL/min of nitrogen

and 2h of desorption time. The switch from chemisorption to desorption was carried out at a heating rate of 10°C/min under nitrogen flow in all cases. The activated carbons were designated by the chemisorption temperature, desorption temperature and the number of cycles used, e.g. for the activated carbon sample 200-500 C2 chemisorption was carried out at 200°C, desorption at 500°C and two chemisorption-desorption cycles were completed.

### **3. Results and Discussion**

#### **3.1 *Activation conditions***

The purpose of the chemisorption step in this cyclic activation approach is the uptake of oxygen that can then be released combined with carbon in the subsequent desorption stage, thus leading to porosity development. The study of the chemisorption step addressed to maximize the oxygen uptake, which would result, as a general trend, in higher burn-off and porosity development per cycle [10].

Isothermal TGA runs with char were carried out in nitrogen and air between 140 and 300°C until constant weight. The yield in inert atmosphere decreased as temperature increased due to the loss of volatile compounds remaining in the char after pyrolysis, as well as adsorbed moisture. In the TGA runs in air, this devolatilization takes place together with oxygen chemisorption and simultaneous desorption of oxygen species. The difference between the yield of isothermal TGA runs in air and the yield of isothermal TGA runs in nitrogen provides information about the balance between oxygen chemisorption and burn-off during chemisorption (Figure 1). Beyond 200°C the difference did not increase significantly, probably due increased evolution of uptaken oxygen and release of volatiles. Working temperatures within the 200-300°C range lead to net weight gains around 2%, referred to the initial char weight (dry basis). In previous works on the application of cyclic activation to waste tires rubber char, yield values above 100% were obtained for TGA runs in air since the much lower porosity of such chars may lead to lower retention of volatile compounds [5, 10]. In the current case the temperature range between 200 and 300°C was identified as the most favorable for carrying out chemisorption. Likewise, the isothermal TGA experiments carried out in

air atmosphere showed that after 120 minutes chemisorption is completed and no further change in weight takes place, therefore this chemisorption time was selected for the activation study.

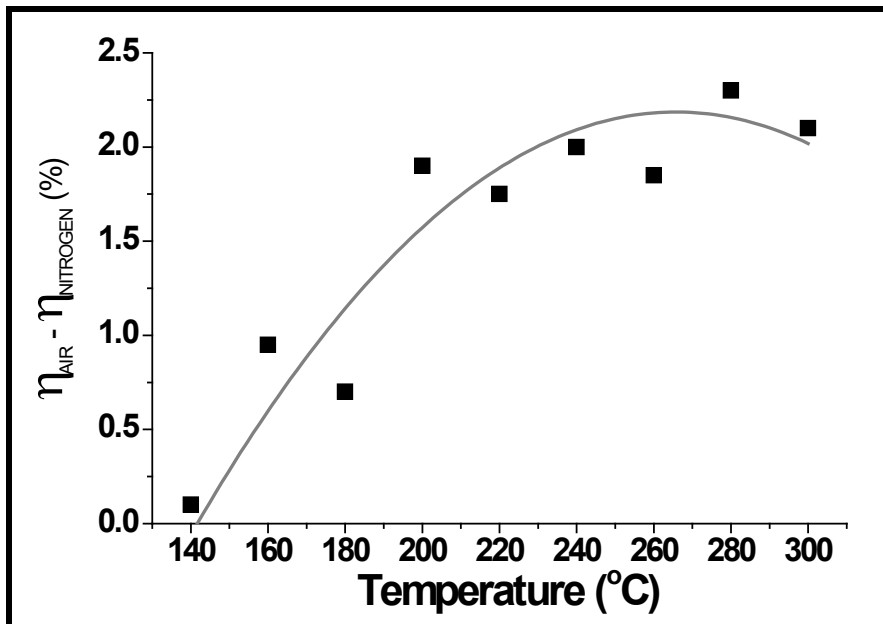


**Figure 1.** Difference between the TGA yield in air and the TGA yield in nitrogen at different temperatures (%w, dry initial char basis).

Although the whole range of chemisorption temperature between 200 and 300°C seems convenient from the point of view of oxygen uptake, different oxygen species may be generated at different chemisorption temperatures. TPD was carried out to analyze the evolution of oxygen species generated at chemisorption temperatures between 200 and 300°C in comparison to the char (Figure 2), showing a different nature of the surface oxygen groups generated upon oxygen chemisorption. Chemisorption above 250°C leads to a TPD profile where the peak around that temperature is missing, indicating a lower presence of carboxylic acid groups. On the contrary, for a chemisorption temperature above 250°C the contribution of groups that evolve as CO<sub>2</sub> upon TPD within the 600-700°C range is higher, whereas the evolution of CO increases in the whole temperature range.

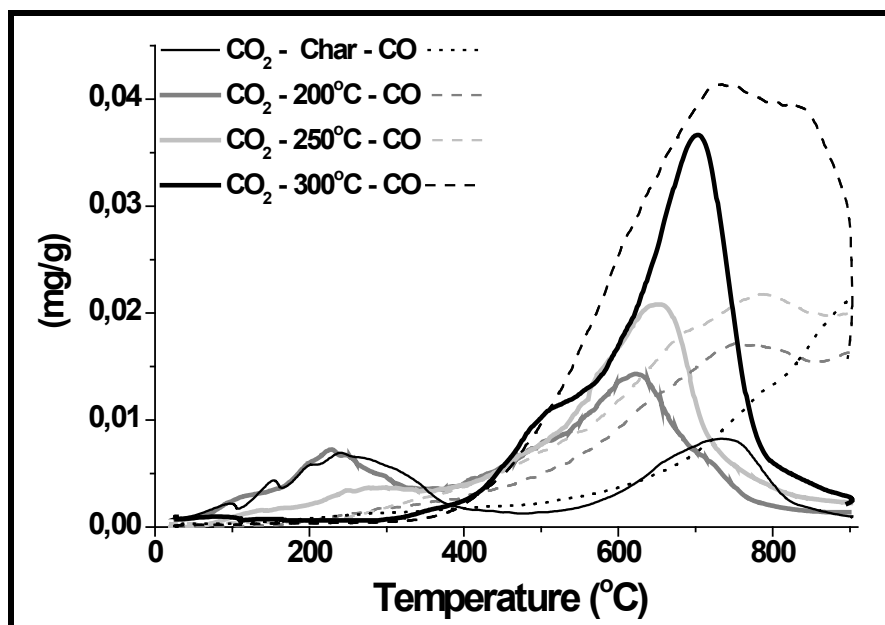


**Figure 2.** TPD profiles of original char and after oxygen chemisorption at 200, 250 and 300°C.

The TPD profiles also provide relevant information about the desorption step of the activation cycles. As can be seen in Figure 2, the oxygen chemisorbed within the 200-250°C range has a high stability upon heating. At 500°C only 30-40% of the CO<sub>2</sub>-evolving groups are desorbed, that evolution being assessed mainly to carboxylic acid and carboxylic anhydride groups [11, 12].

Likewise, around 900°C, the desorption of CO<sub>2</sub> evolving groups is virtually completed, with a maximum in the TPD profile around 675°C, which can be attributed to lactones [11, 12]. The stability of the oxygen groups is higher for the species that evolve as CO. In this case the amount evolved peaks at 800°C, probably due to the decomposition of carbonyl and quinone groups.

With the view in the activation of the char, a chemisorption temperature of 300°C is not advisable, since a substantial part of the uptaken oxygen can only be desorbed at high temperatures, which is a limitation for burn-off and porosity generation. Taking into account the results of Figures 1 and 3, temperatures of 200, 250 and 275°C were selected for the chemisorption step. Likewise, values of 500, 675, 850 and 950°C were selected for the desorption step of the activation cycles.



### 3.2. Influence of activation conditions

Under all the combinations of chemisorption and desorption temperatures studied, the burn-off increased almost linearly with the number of activation cycles (Figure 3). As a general trend, burn-off increased with chemisorption and desorption temperature, thus the highest burn-off was observed for the series prepared at a chemisorption temperature of 275°C with a desorption temperature of 950°C.

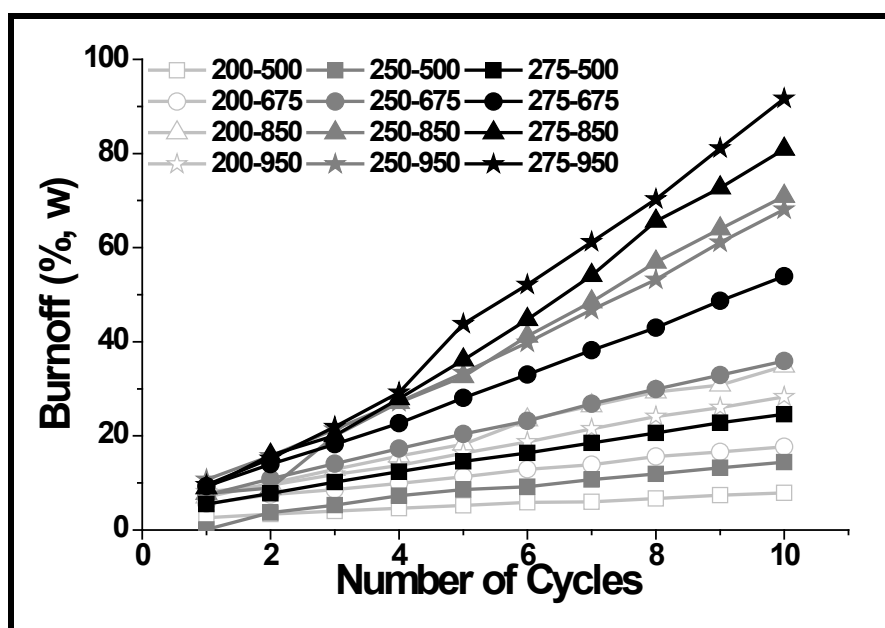


**Figure 3.** Burn-off vs number of activation cycles at different activation conditions.

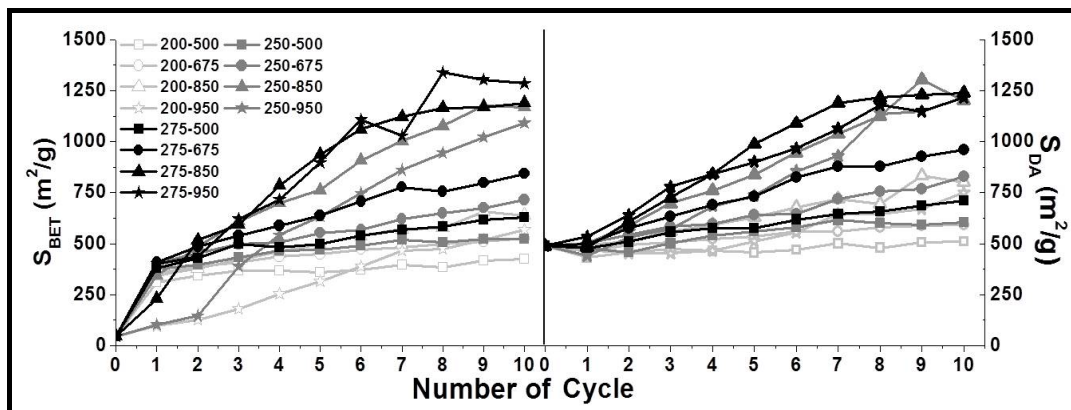
The starting char used in this work was mainly microporous with a  $S_{\text{BET}}$  of  $47\text{m}^2/\text{g}$  and a  $S_{\text{DA}}$  of  $505\text{m}^2/\text{g}$  [6]. Due to the narrow nature of the microporosity of the char, the porosity of the resulting activated carbons was analyzed by both the BET and Dubinin-Astakhov methods.

The Dubinin-Radushkevich and Dubinin-Astakhov equations have been used to describe the filling of micropores and the energetic heterogeneity of the solids. While several studies [13, 14] postulated that the Dubinin-Radushkevich equation applies only to solids with a uniform structure of micropores, others [15-19] proposed a modification of this equation when a microporous solid possesses micropores of the same shape but of different sizes. One of those modifications is the Dubinin-Astakhov equation, which

can be applied to the description of the adsorption onto structurally heterogeneous solids [8, 20]. In this work the Dubinin-Astakhov method has been used because of the heterogeneous structure of the samples and the better correlation coefficient obtained in all cases.

The development of surface area with the number of cycles performed is depicted in Figure 4. For most of the samples an important development of porosity in terms of  $S_{\text{BET}}$  was observed in the first cycle, in all cases due to the widening of previously existing narrow micropores, since the  $S_{\text{DA}}$  values hardly increased, even decreased, after the first cycle. A monotonical increase of surface area was in general observed throughout the following cycles, which was more significant when combining the highest chemisorption and desorption temperatures. This is consistent with the higher burn-off values achieved (see Figure 3). As a general trend, the  $S_{\text{DA}}$  values are higher than the  $S_{\text{BET}}$  ones upon the successive cycles indicating that the development of porosity proceeds through the creation of new micropores in addition to the widening of existing ones.

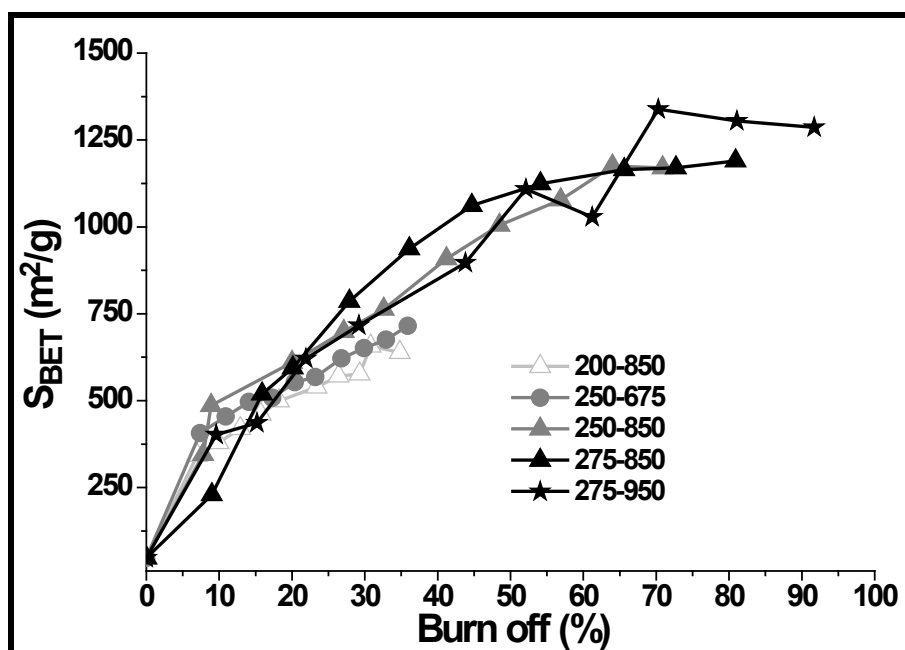
The highest development of surface area corresponds to a chemisorption temperature of 275°C combined with a desorption temperature of 950°C (1339 m<sup>2</sup>/g, sample 275-950 C8). It can also be observed that under those conditions the development of porosity is very low in the last cycles and even a decrease of surface area occurs. This observation may be interpreted in terms of the collapse of pores taking place at high burn-off (c.a. 70%), as it has been reported for the physical activation of other carbonaceous materials [21]. Likewise, Polyakov et al. [22] suggested that thermal stress induced a collapse of the microporous structure leading to the formation of mainly mesopores.



**Figure 4.**  $S_{\text{BET}}$  and  $S_{\text{DA}}$  vs number of cycles for 10-cycle test at different conditions.

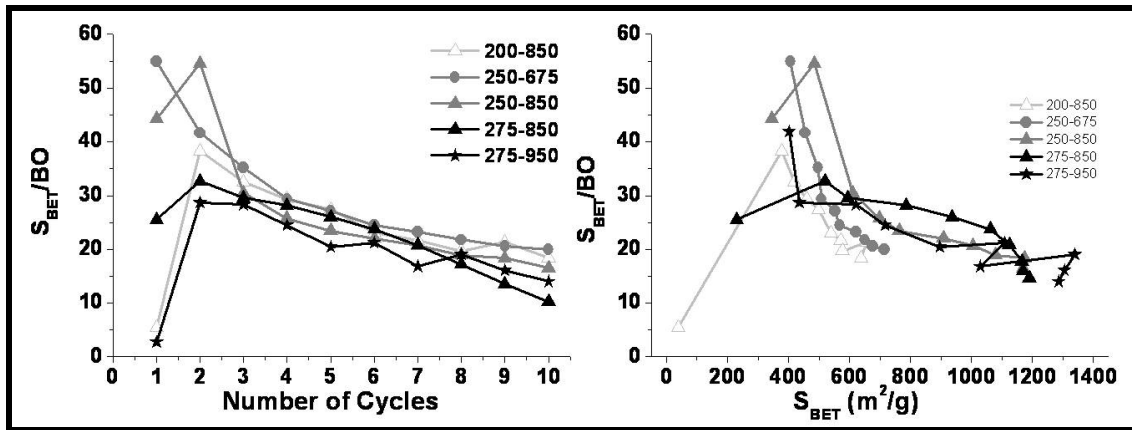
Previous studies about the preparation of activated carbon from grape seeds reported  $S_{BET}$  values around 400-500m<sup>2</sup>/g with a burn-off of 75% by one-step pyrolysis/activation at 800°C with steam [23]. Savova et al. [24] obtained a granular activated carbon from grape seeds with heterogeneous pore size distribution with macropore, mesopore and micropore volumes of 0.28, 0.18 and 0.12cm<sup>3</sup>/g, respectively. In the current work similar results are obtained within the micropore range after 1-2 activation cycles and a burn-off between 10-15%, depending of the activation conditions. This feature of cyclic activation is relevant for the sake of preservation of the particle integrity.

Figure 5 shows that the surface area generated per burn-off unit, is quite different depending on the activation conditions, particularly in the first activation cycles. Thus, activated carbons with values of  $S_{BET}$  between 600 and 750m<sup>2</sup>/g can be obtained at burn-offs between 25 and 35%, depending on the activation conditions. Due to the different burn-off per cycle,  $S_{BET}$  values of 750m<sup>2</sup>/g are achieved after 4-5 cycles for combinations of high chemisorption and desorption temperatures whereas up to 10 cycles are needed for combinations of low chemisorption and desorption temperatures.



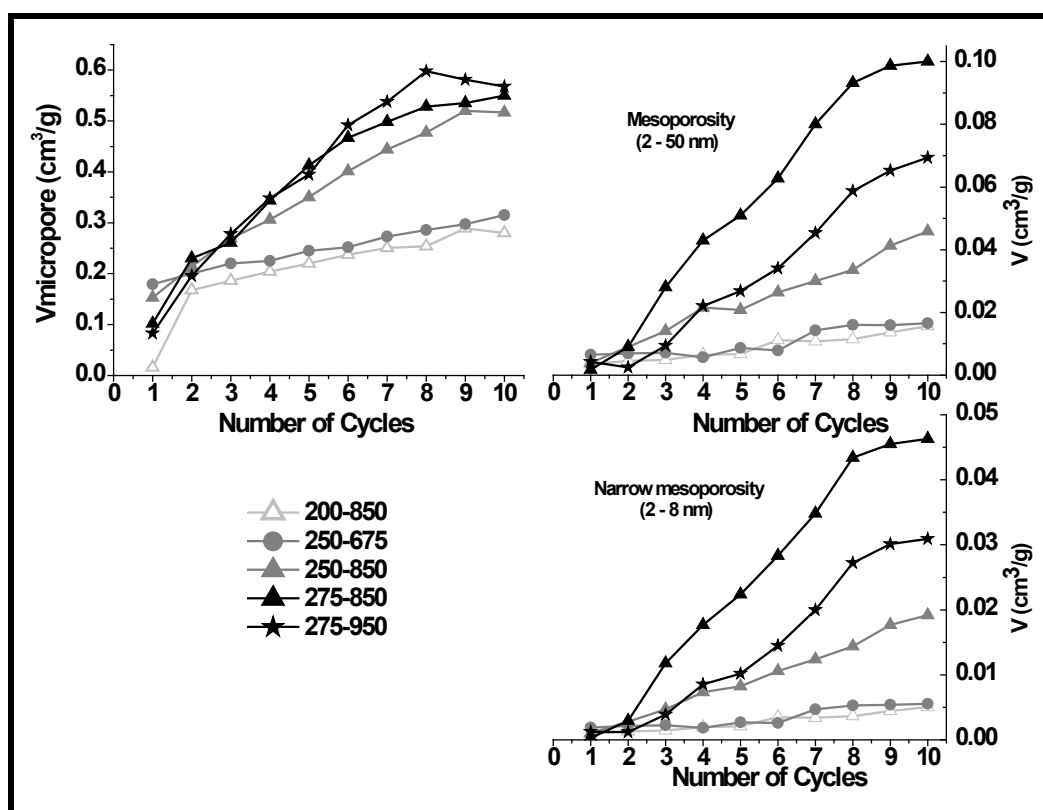
**Figure 5.** Variation of  $S_{BET}$  versus burn-off.

Figure 6 shows the development of  $S_{\text{BET}}$  per unit of burn-off along the 10-cycles test (a) and versus  $S_{\text{BET}}$  (b). It can be seen that the most important factor in that respect is the chemisorption temperature. Thus, at low chemisorption temperatures burn-off leads to a higher generation of porosity per unit of surface area. The differences with the results for higher chemisorption temperatures become smaller as the number of cycles and the surface area developed increase. The amount and location of the oxygen surface groups formed at different chemisorption temperature may be responsible for the distinct generation of porosity.



**Figure 6.** Variation of  $S_{\text{BET}}/\text{burn-off}$  versus number of cycles (a) and  $S_{\text{BET}}$  (b) at different activation conditions.

The different response to the activation conditions is also of great interest for the preparation of activated carbons with different properties, as can be seen in Figure 7, where the evolution of micropore and mesopore volume along the cycles is shown. The resulting activated carbons are in all the cases essentially microporous solids with a fairly low contribution of mesopores that only for the samples obtained combining the highest chemisorption and desorption temperatures has some significance, always modest. The development of mesopores is only significant after 2 - 3 cycles, which is in agreement with a mesopore formation mechanism based on the widening of previously created micropores [25]. Thus, mesoporosity development was observed once the activated carbons achieved a micropore volume of around  $0.25\text{cm}^3/\text{g}$ . After 10 activation cycles the samples of higher porosity ( $V_{\text{micro}}: 0.57\text{cm}^3/\text{g}$ ) showed a mesopore volume close to  $0.1\text{cm}^3/\text{g}$ .



**Figure 7.** Pore volume development from N<sub>2</sub> isotherms along the cycles at different activation conditions.

In an additional set of experiments the  $S_{\text{BET}}$  and  $S_{\text{DA}}$  were measured both after the chemisorption and after the desorption step of each cycle for the 200-950 and the 275-950 series (Figure 8). The results confirm that the development of porosity takes place in the desorption step of each cycle, whereas oxygen chemisorption provokes in general no significant modification of surface area at the highest temperature tested (275°C), and even a considerable decrease at the lowest temperature (200°C), which can be associated to the location of oxygen at the pore mouths thus restricting the access of nitrogen in the  $S_{\text{BET}}$  determination. Such trend is not observed at a chemisorption temperature of 275°C (series 275-950) due to earlier development of wider pores, as it was discussed above. The comparison of the results in Figure 8 and 4 also shows the good reproducibility of the method.

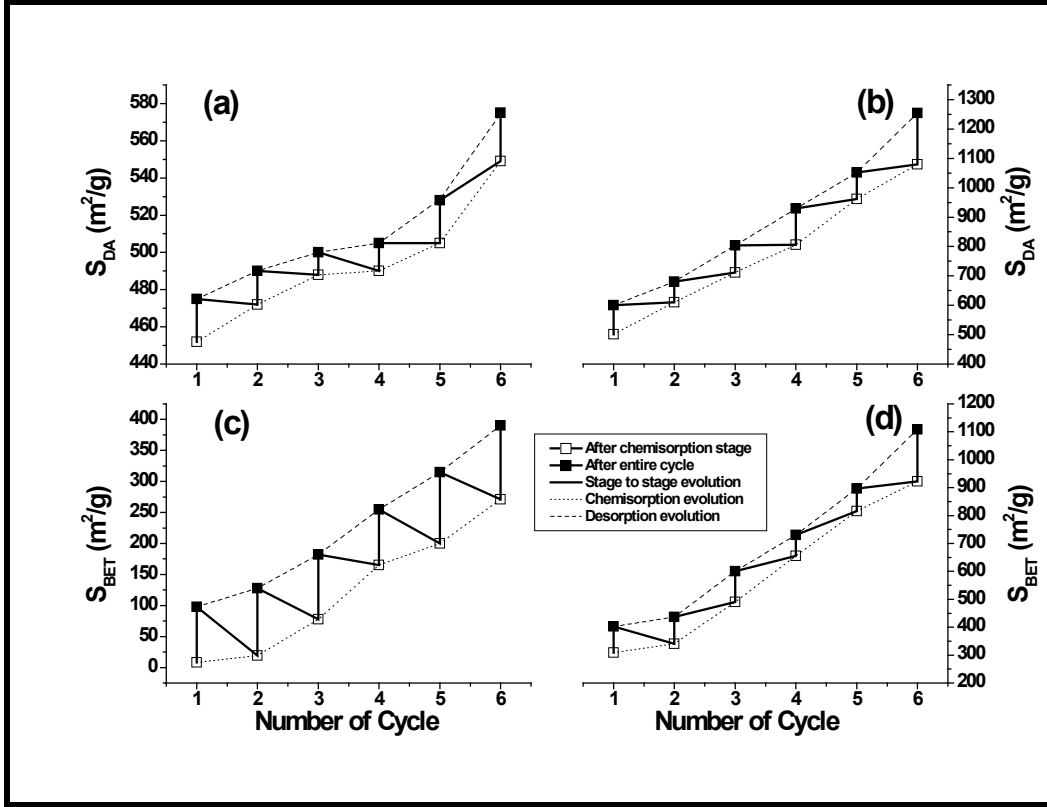


**Figure 8.** Evolution of  $S_{BET}$  and  $S_{DA}$  versus number of cycles after chemisorption step and the entire cycle for the 200-950 (a and c) and 275-950 series (b and d).

The pore size distribution (PSD) is a key element in the characterization of porous carbons and a number of methods have been developed for the PSD analysis, the non-local density functional theory (NLDFT) being widely used for the characterization of the pore structure of activated carbons and other porous materials [9]. However, global parameters such as the mean pore size are also commonly used to evaluate the type of porosity. Figure 9a shows that the mean micropore width increases with the number of cycles, which is in agreement with the aforementioned widening of existing pores, the mean micropore width being higher for combinations of high chemisorption and desorption temperatures. On the opposite the mean width of mesopores decreases along the reaction cycles up to the lowest range from burn-offs of about 30%. The effect of operating conditions on the mean width of mesopores is almost negligible. The decrease of mesopore width can be interpreted in terms of the creation of narrow mesopores as a result of micropores widening. Thus, the mesopore mean width remains higher for the

activation conditions identified as less favorable for the development of mesoporosity (Figure 8), i.e. low chemisorption and desorption temperatures.

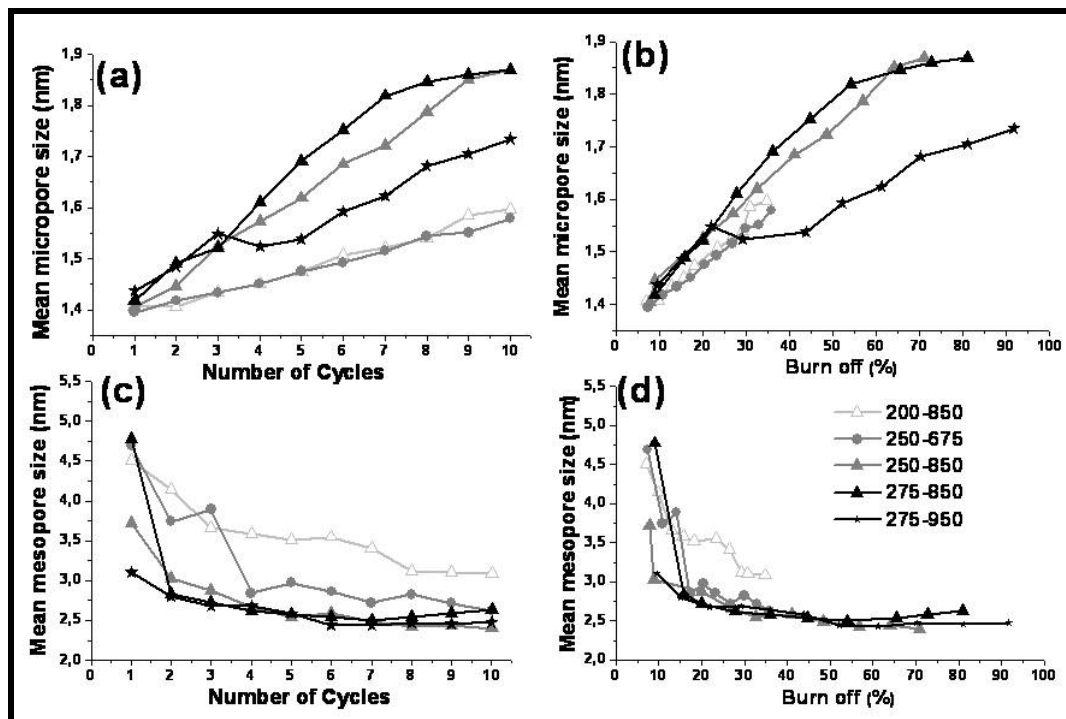


**Figure 9.** (a) and (b) mean micropore width versus number of cycles and burn-off. (c) and (d) mean mesopore width versus number of cycles and burn-off.

In order to have a deeper knowledge on the generation of porosity, the micropore size distribution was calculated from CO<sub>2</sub> isotherms and the mesopore size distribution from N<sub>2</sub> isotherms by the NLDFT method for five activated carbons prepared in different conditions but all of them with S<sub>BET</sub> around 700-800 m<sup>2</sup>/g and burn-off around 30% (Figure 10). As can be observed, the microporosity pattern is quite similar for all the samples, with a fairly homogeneous distribution characterized by three important contributions centered at 0.45, 0.55 and 0.88 nm in all cases, even for the char. However, regarding the mesopore distributions there are significant differences between the samples prepared upon 4 activation cycles at more severe conditions and the samples prepared upon 8-9 cycles at milder conditions, and it can be seen that the char has no significant mesoporosity. Thus, the contribution of narrow mesoporosity is much lower for the 8 and 9 cycles samples, being essentially microporous and good candidates for their application as molecular sieves. For the 4-cycles a higher

development of wide microporosity and narrow mesoporosity centered at 2.2 nm can be observed. Finally, no significant differences can be found in the pattern of mesoporosity within the 8-50 nm range, being this porosity probably already present in the starting char.

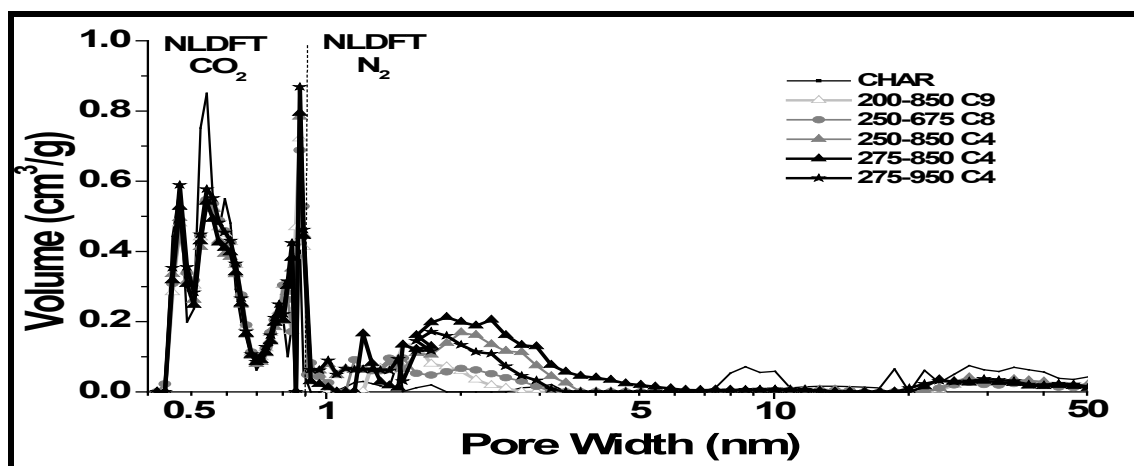


**Figure 10.** Pore size distribution by NLDFT method from CO<sub>2</sub> (0.4-0.9 nm) and N<sub>2</sub> (0.9-50 nm) isotherms for selected samples.

Figures 11 and 12 show the macropore volume determined by mercury porosimetry for all the activated carbon series after cycle number 10. As a general trend, the generation of macroporosity increases with both chemisorption and desorption temperature. The macropore volume generated correlates well with burn-off, showing little influence of the activation conditions. Thus, whereas activation conditions are important for both the type and amount of pores generated in the micro and mesopore range, they do not seem to have noticeable influence on the pore distribution within the macropore range.



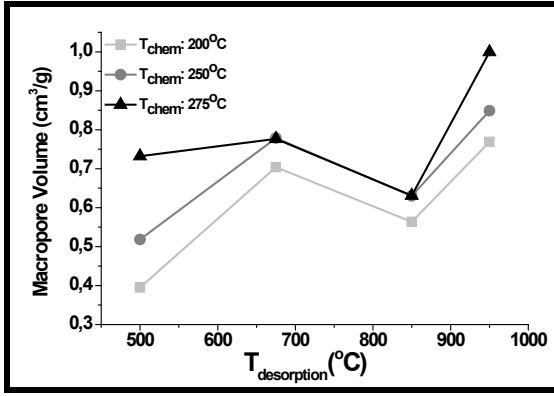


**Figure 11.** Macropore volume ( $4 \mu\text{m} > d > 0.05 \mu\text{m}$ ) for all AC series after cycle 10.

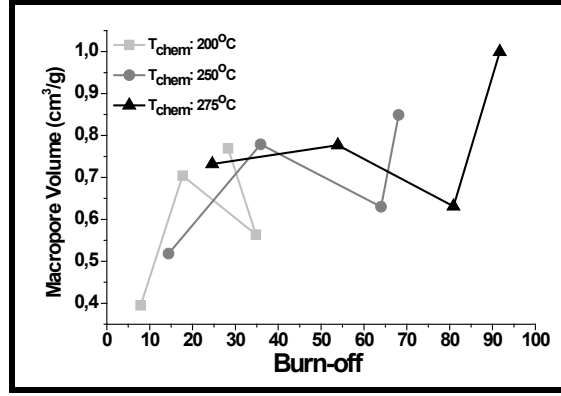


**Figure 12.** Macropore volume ( $4 \mu\text{m} > d > 0.05 \mu\text{m}$ ) for all AC series after cycle 10.

To provide a more complete sight on meso and macroporosity, pore size distribution of the activated carbons within the  $0.01 \mu\text{m}$  to  $4 \mu\text{m}$  range is depicted in Figure 13. As can be observed all the samples showed an equivalent pattern in the macropore range, being the pore volume in the mesopore range negligible in comparison with that of macropores.

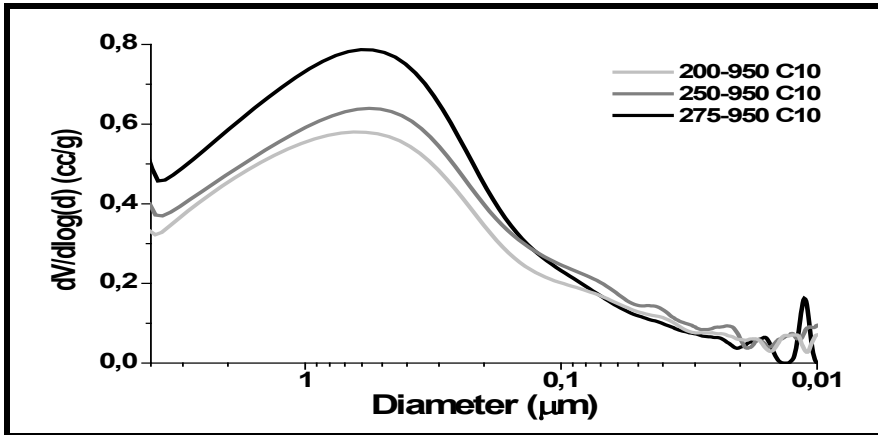


**Figure 13.** Macropore and mesopore size distribution for 200-950 C10, 250-950 C10 and 275-950 C10 samples.

### 3.3. Comparison with results in literature

In Figure 14 the results of  $S_{\text{BET}}$  vs burn-off are compared with the reported by other authors from physical activation of other agricultural by-products like apricot stones

[24], cherry stones [24], olive stones [1], pecan shells [26], coconut shells [21] and other biomass residues, activated with steam [1, 24, 27-31] and CO<sub>2</sub> [1, 21, 31-36]. It can be observed that the surface area values obtained by oxygen chemisorption–desorption of grape seeds covers the usual range of porosity for activated biomass materials, and that such porosity development can be achieved at burn-off values below the average results. Thus, cyclic activation by chemisorption/desorption allows overcoming the drawback of low development of porosity characteristic of oxygen when used in conventional activation.

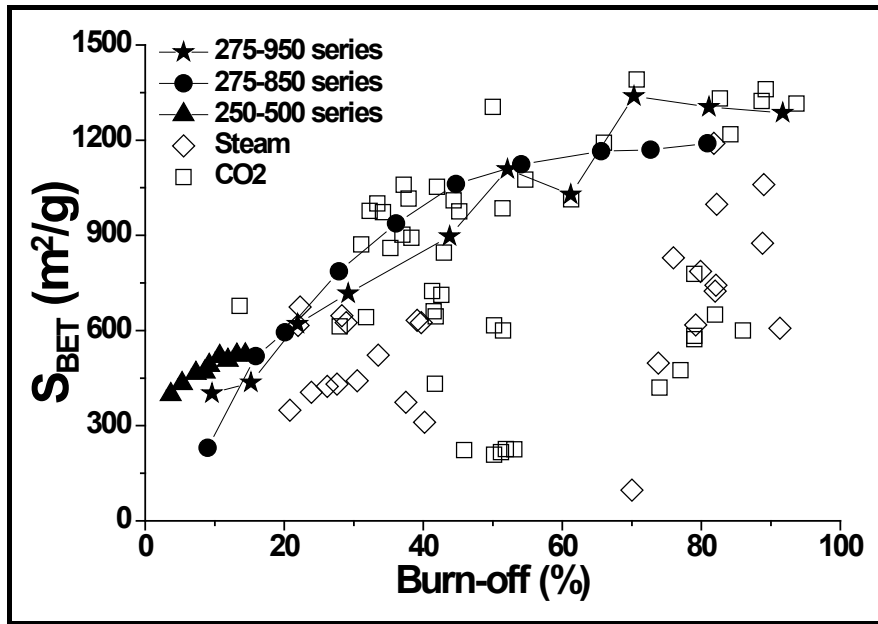


**Figure 14.** Comparison of  $S_{BET}$  vs Burn-off from oxygen cyclic chemisorption/desorption activation (current work) with literature results on the activation of biomass residues [1, 21, 24, 26-36].

### 3.4 *Morphology study by Scanning Electron Microscopy*

The morphology of the activated carbons was evaluated by SEM, showing as the most relevant result that the granular morphology of the starting char is maintained along the activation cycles due to the controlled burn-off (Figure 15). Burn-off seems to take place preferentially at the outer layer of the particles, as can be inferred from the size reduction observed in Figure 15. Likewise, changes in the texture can be observed with a higher occurrence of large macropores, cracks and channels as the number of cycles is increased.

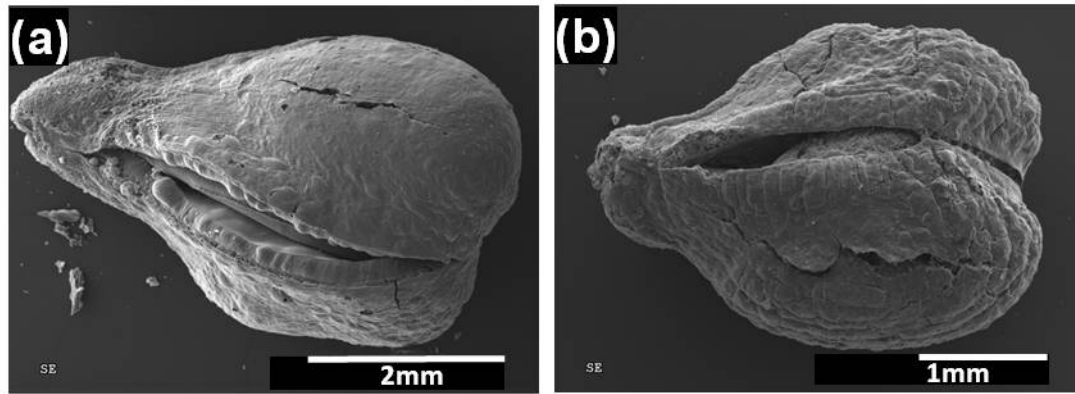


**Figure 15.** SEM micrographs of (a) 275-850 C5 sample. (b) 275-850 C10 sample.

Figure 16 shows the SEM images of crushed particles showing the egg shell structure of the activated carbon particles resulting from the volatilization of the albumen and embryo during the pyrolysis stage. It can be observed that after 10 activation cycles both the outer layer and the carbonized tissue in the inner of the particle have been partially removed compared with the char SEM images (Figure 17). This indicates some homogeneity in the oxidation and burn-off resulting from the low temperature and long time of the chemisorption stage. The activated carbon obtained has most of the carbonaceous material allocated in a shell thickness of around 250 $\mu$ m, which is of great interest since the granular material prepared can combine easy handling and low pressure loss for packed bed applications with convenient mass transfer due to short diffusion path.

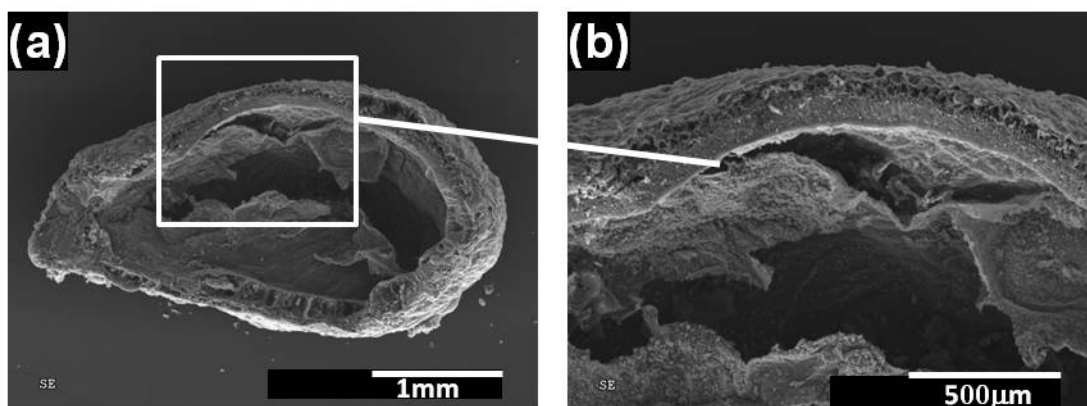


**Figure 16.** SEM micrographs of (a) Cross section of 275-850 C10 sample. (b) Detail of wall from 275-850 C10 sample.

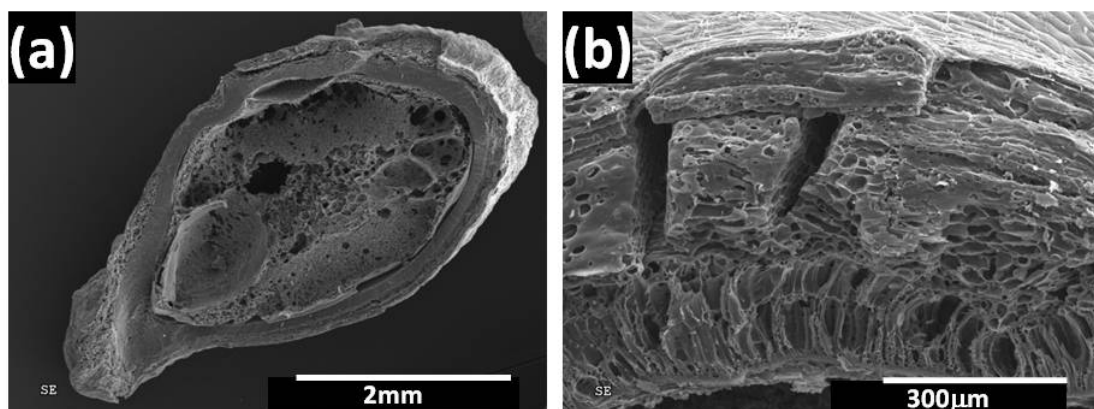


**Figure 17.** a) Cross section of a grape seed char. b) Carbonized seed coat (char).

To study the pore structure of the different layers of the activated carbon particles 200-950 C4 and 275-950 C4 samples were subjected to attrition in a vibrating sifter. These samples are representative of the different materials that can be obtained by the use of different activation conditions. The samples also have a suitable balance between surface area and burn-off, so that the integrity and strength of the particles can be preserved. During the attrition test the first fraction of the fines generated and passing through the sieve openings ( $<1$  mm) was collected after 2h testing time. A total of five fractions were collected at regular intervals of 2h. The results in Table 1 show a rather homogeneous development of surface area throughout the particle wall. The most noticeable differences can be found for  $S_{BET}$ , thus for the two samples studied the inner layers show significantly lower values of  $S_{BET}$ , suggesting the preferential generation of narrow porosity in the outer layers. In the case of microporosity ( $S_{DA}$ ) also preferential development of porosity is observed at the outer layers, the differences being higher for 275-950 C4.

It is also remarkable that the activated carbon particles have a good resistance to attrition, since only 2.2% of the initial mass was lost in the first 2h of the test. The strength of the particles is of great importance for the sake of handling and performance in potential applications. The strength of the outer layers seems to be homogeneous according to the similar loss of mass upon 2h shaking.

\* Corresponding author Tel.: +34 914978051; fax: +34 914972981.

E-mail address: fran.heras@uam.es

**Table 1.** Micropore and mesopore surface area and mass-loss of 200-950 C4 and 275-950 C4 samples.

<b>SAMPLE</b>	<b>S<sub>BET</sub> (m<sup>2</sup>/g)</b>	<b>S<sub>DA</sub> (m<sup>2</sup>/g)</b>	<b>Mass loss (%)</b>
<b>200-950 C4</b>	<b>255</b>	<b>482</b>	
<b>Fraction 1</b>	<b>169</b>	<b>567</b>	<b>2.2</b>
<b>Fraction 2</b>	<b>208</b>	<b>610</b>	<b>2.2</b>
<b>Fraction 3</b>	<b>227</b>	<b>636</b>	<b>1.8</b>
<b>Fraction 4</b>	<b>207</b>	<b>580</b>	<b>2.2</b>
<b>Fraction 5</b>	<b>188</b>	<b>557</b>	<b>2.2</b>
<b>Final sample</b>	<b>84</b>	<b>475</b>	

<b>SAMPLE</b>	<b>S<sub>BET</sub> (m<sup>2</sup>/g)</b>	<b>S<sub>DA</sub> (m<sup>2</sup>/g)</b>	<b>Mass loss (%)</b>
<b>275-950 C4</b>	<b>717</b>	<b>868</b>	
<b>Fraction 1</b>	<b>543</b>	<b>845</b>	<b>3.0</b>
<b>Fraction 2</b>	<b>560</b>	<b>750</b>	<b>3.0</b>
<b>Fraction 3</b>	<b>655</b>	<b>858</b>	<b>2.6</b>
<b>Fraction 4</b>	<b>646</b>	<b>812</b>	<b>2.5</b>
<b>Fraction 5</b>	<b>597</b>	<b>783</b>	<b>2.5</b>
<b>Final sample</b>	<b>429</b>	<b>599</b>	

#### 4. Conclusions

The influence of operating conditions on the activation of grape seeds by cyclic oxygen chemisorption/desorption was investigated. The procedure proposed permits a controlled development of porosity with low burn-off maintaining the integrity of the particles. A fast increase of S<sub>BET</sub> was achieved in the two first cycles, and then a monotonically increase was observed in successive cycles. The highest values of burn-off, S<sub>BET</sub> and S<sub>DA</sub> were obtained by combining high temperatures of chemisorption and desorption (275-850°C and 275-950°C) especially for 275-950 C8 sample with specific surface values of 1339 and 1219m<sup>2</sup>/g for S<sub>BET</sub> and S<sub>DA</sub>, respectively. Although, low chemisorption temperatures lead to a higher generation of porosity per burn-off unit. The activation led essentially to the development of microporosity and macroporosity, being the mesopore volume in general low and only significant in the case of the samples obtained for combination of high chemisorption and desorption temperatures.

SEM characterization showed that the activated carbon maintained the morphology of the seeds even after 10 cycles, with an egg shell structure interesting for the sake of application. The activation conditions can be adjusted to provide an appropriate balance between surface area and burn-off, which enables to obtain porous granular materials with relevant strength.

## 5. Acknowledgment.

The authors greatly appreciate financial support from the Spanish Ministerio de Ciencia e Innovación (CTQ2009-09983).

## 6. References

- [1] A.H. El-Sheikh, A.P. Newman, H.K. Al-Daffae et al. Characterization of activated carbon prepared from a single cultivar of Jordanian Olive stones by chemical and physicochemical techniques. *J. Anal. Appl. Pyrolysis* 71 (2004) 151-164.
- [2] A. Molero Gómez, C. Pereyra López, E. Martínez de la Ossa. Recovery of grape seed oil by liquid and supercritical carbon dioxide extraction: a comparison with conventional solvent extraction. *Chem. Eng. J.* 61 (1996) 227-231.
- [3] J.M. Luque-Rodríguez, M.D. Luque de Castro, P. Pérez-Juan. Extraction of fatty acids from grape seed by superheated hexane. *Talanta* 68 (2005) 126-130.
- [4] X. Py, A. Guillot, B. Cagnon. Activated carbon porosity tailoring by cyclic sorption/decomposition of molecular oxygen. *Carbon* 41 (2003) 1533.
- [5] F. Heras, N. Alonso-Morales, D. Jiménez-Cordero, M.A. Gilarranz, J.J. Rodríguez. Granular mesoporous activated carbons from waste tires by cyclic oxygen chemisorption-desorption. *Ind. Eng. Chem. Res.* 51 (2012) 2609-2614.
- [6] D. Jiménez-Cordero, F. Heras, N. Alonso-Morales, M.A. Gilarranz, J.J. Rodríguez. Porous structure and morphology of granular chars from flash and conventional pyrolysis of grape seeds. *Biomass Bioenergy* 2013; 54: 123-132.
- [7] S. Brunauer, E. Emmett, E. Teller. Adsorption of gases in multimolecular layers. *The J. Am. Chem. Soc.* 60 (1938) 309-319.
- [8] A. Gil, P. Grange. Application of the Dubinin-Radushkevich and Dubinin-Astakhov equations in the characterization of microporous solids. *Colloids Surf A Physicochem. Eng. Asp.* 113 (1996) 39-50.

- [9] J. Jagiello, M. Thommes. Comparison of DFT characterization methods based on N<sub>2</sub>, Ar, CO<sub>2</sub> and H<sub>2</sub> adsorption applied to carbons with various pore size distributions. *Carbon* 42 (2004) 1227-1232.
- [10] F. Heras, N. Alonso-Morales, M.A. Gilarranz, J.J. Rodríguez. Activation of waste tire char upon cyclic oxygen chemisorption-desorption. *Ind. Eng. Chem. Res.* 48 (2009) 4664 – 4670.
- [11] J.L. Figueiredo, M.F.R. Pereira. The role of surface chemistry in catalysis with carbons. *Catal. Today* 150 (2010) 2-7.
- [12] S.A.C. Carabineiro, T. Thavorn-amornsi, M.F.R. Pereira, P. Serp, J.L. Figueiredo. Comparison between activated carbon, carbon xerogel and carbon nanotube for the adsorption of the antibiotic ciprofloxacin. *Catal. Today* 186 (2012) 29-34.
- [13] H.F. Stoeckli. A generalization of the Dubinin—Radushkevich equation for the filling of heterogeneous micropore systems. *J. Colloid Interface Sci.* 59 (1977) 184–185.
- [14] M. Jaroniec, J. Piotrowska. Isotherm equations for adsorption on heterogeneous microporous solids. *Monatsh. Chem.* 117 (1986) 7-19.
- [15] A. Gil, M. Montes. Analysis of the microporosity in pillared clays. *Langmuir* 10 (1994) 291-297.
- [16] M. Jaroniec, J. Choma. On the characterization of structural heterogeneity of microporous solids by discrete and continuous micropore distribution functions. *Mater. Chem. Phys.* 19 (1988) 267-289.
- [17] M.M. Dubinin. Inhomogeneous microporous structures of carbonaceous adsorbents. *Carbon* 19 (1981) 321-324.
- [18] M. Rodwadowski, R. Wojsz. An attempt at determination of the structural heterogeneity of microporous adsorbents. *Carbon* 22 (1984) 363-367.
- [19] M. Jaroniec, R.K. Gilpin, K. Kaneko. Evaluation of energetic heterogeneity and microporosity of activated carbon-fibers on the basis of gas-adsorption isotherms. *Langmuir* 7 (1991) 2719-2722.

- [20] M. Carrasco-Marin, M.V. Lopez-Ramon, C. Moreno-Castilla. Applicability of the Dubinin-Radushkevich equation to carbon dioxide adsorption on activated carbons. *Langmuir* 9 (1993) 2758-2760.
- [21] S. Guo, J. Peng, W. Li et al. Effects of CO<sub>2</sub> activation on porous structures of coconut shell-based activated carbons. *Appl. Surf. Sci.* 255 (2009) 8443-8449.
- [22] M. Polyakov, M. Poisot, W.E. Maurits, T. Drescher, A. Lotnik, L. Kienle, W. Bensch, M. Muhler, W. Grunert. Carbon-stabilized mesoporous MoS<sub>2</sub> - Structural and surface characterization with spectroscopic and catalytic tools. *Catal. Commun.* 12 (2010) 231-237.
- [23] K. Gergova, N. Petrov, S. Eser. Adsorption properties and microstructure of activated carbons produced from agricultural by-products by steam pyrolysis. *Carbon* 32 (1994) 693-702.
- [24] D. Savova, E. Apak, E. Ekinici, F. Yardim, N. Petrov, T. Budinova, M. Razvigorova, V. Minkova. Biomass conversion to carbon adsorbents and gas. *Biomass Bioenergy* 21 (2001) 133-142.
- [25] R. Mysyk, Q. Gao, E. Raymundo-Piñero, F. Béguin. Microporous carbons finely-tuned by cyclic high pressure low-temperature oxidation and their use in electrochemical capacitors. *Carbon* 50 (2012) 3367-3374.
- [26] M. Admedna, W.E. Marshall, R.M. Rao. Production of granular activated carbons from select agricultural by-products and devaluation of their physical, chemical and adsorption properties. *Bioresour. Technol.* 71 (2000) 113-123.
- [27] B.S. Girgis, S.S. Yunis, A.M. Soliman. Characteristics of activated carbon from peanut hulls in relation to conditions of preparation. *Mater. Lett.* 57 (2002) 164-172.
- [28] M. Fan, W. Marshall, D. Dugaard, R.C. Brown. Steam activation of chars produced from oat hulls and corn stover. *Bioresour. Technol.* 93 (2004) 103-107.
- [29] A-NA. El-Hendawy, S.E. Samra, B.S. Girgis. Adsorption characteristics of activated carbons obtained from corncobs. *Colloids Surf A Physicochem. Eng. Asp.* 180 (2001) 209-221.



- [30] M. Ahmedna , W.E. Marshall, A.A. Husseiny, R.M. Rao, I. Goktepe. The use of nutshell carbons in drinking water filters for removal of trace metals. *Water Res.* 38 (2004) 1062-1068.
- [31] L.H. Wartelle, W.E. Marshall, C.A. Toles, et al. Comparison of nutshell granular activated carbons to commercial adsorbents for the purge-and-trap gas chromatographic analysis of volatile organic compounds. *J. Chromatogr. A* 879 (2000) 169-175.
- [32] A.C. Lua, T. Yang, J. Guo. Effects of pyrolysis conditions on the properties of activated carbons prepared from pistachio-nut shells. *J. Anal. Appl. Pyrolysis* 72 (2004) 279-287.
- [33] A. Marcilla, S. Garcia-Garcia, M. Asensio, J.A. Conesa. Influence of thermal treatment regime on the density and reactivity of activated carbons from almond shells. *Carbon* 38 (2000) 429 - 440.
- [34] E. Iniesta, F. Sanchez, A.N. Garcia, et al. Influence of the holding temperature of the first heating step in a two-heating step carbonization process on the properties of chars and activated carbons from almond shells. *J. Anal. Appl. Pyrolysis* 58 (2001) 967-981.
- [35] T. Zhang, W.P. Walawender, L.T. Fan, M. Fan, D. Daugaard, R.C. Brown. Preparation of activated carbon from forest and agricultural residues through CO<sub>2</sub> activation. *Chem Eng J* 105 (2004) 53-59.
- [36] S. Girgis Badie, M. Soliman Ashraf, A. Fathy Nady. Development of micro-mesoporous carbons from several seed hulls under varying conditions of activation. *Microporous Mesoporous Mater.* 142 (2011) 518-525.